



Lithofacies Architecture and Distribution Patterns of Lacustrine Mixed Fine-Grained Rocks –a Case Study of Permian Lucaogou Formation in Jimsar Sag, NW China

Senlin Yin^{1*}, Baiyu Zhu^{1*}, Youxin Wu^{1,2} and Feng Xu³

¹Research Institute of Mud Logging Technology and Engineering, Yangtze University, Jingzhou, China, ²School of Geosciences, Yangtze University, Wuhan, China, ³Research Institute of Exploration and Development, PetroChina Xinjiang Oilfield Company, Karamay, China

OPEN ACCESS

Edited by:

Feng Yang,
China University of Geosciences,
China

Reviewed by:

Hui Han,
Southwest Petroleum University,
China
Nan Xin Yin,
Chongqing University of Science and
Technology, China

*Correspondence:

Senlin Yin
yinxiang_love@qq.com
Baiyu Zhu
631579905@qq.com

Specialty section:

This article was submitted to
Economic Geology,
a section of the journal
Frontiers in Earth Science

Received: 24 September 2021

Accepted: 11 October 2021

Published: 08 November 2021

Citation:

Yin S, Zhu B, Wu Y and Xu F (2021)
Lithofacies Architecture and
Distribution Patterns of Lacustrine
Mixed Fine-Grained Rocks –a Case
Study of Permian Lucaogou Formation
in Jimsar Sag, NW China.
Front. Earth Sci. 9:782208.
doi: 10.3389/feart.2021.782208

As the controlling effect of complex lithofacies of lacustrine mixed fine-grained rocks on the shale oil sweet spot remains unclear, core, outcrop, general logging, nuclear magnetic resonance (NMR) logging, testing, and production data were used to study the types, combination pattern, and genesis of lithofacies architectures of lacustrine mixed fine-grained rocks in the study area by lithofacies hierarchy analysis, X-ray fluorescence (XRF) logging, UAV, and 3D geological modeling. The research shows that: 1) According to lithology and sedimentary structure, the mixed fine-grained rocks can be divided into 13 lithofacies types of different origins in 5 sub-categories and 2 categories. 2) UAV photography was combined with a traditional field survey to characterize the 3D spatial distribution of lithofacies architecture of the Lucaogou Formation on the outcrop, and it is found that the lithofacies architecture patterns of mixed fine-grained rocks include three types: gradual change type, abrupt change type, and special type. The gradual change type with higher sand development degree and symmetrical lithofacies architecture has a high quality reservoir with dissolution pores, and is mixed beach-bar sand in the mixed zone. It is high in development degree and often appears as several similar cycles stacking over each other. The abrupt change type can be subdivided into two sub-types, asymmetric and smaller in reservoir thickness. It is very high in development degree and often comes in several similar cycles. The special type belongs to thick clastic rock relatively independent in the mixed fine-grained rocks with a high development degree of sand. The sand is a higher quality reservoir with properties of tight reservoir. It often appears as stacking of single cycle sand. 3) The different lithofacies architectures in the mixed fine-grained rocks have significant differences in distribution. The gradual change type is mainly composed of mudstone, dolomitic siltstone, and sandy dolomite, dolomitic siltstone, and mudstone, and appears in lenticular shape overlapping with each other on the plane. The abrupt change type is made up of felsic siltstone, dolomitic siltstone, sandy dolomite, and mudstone, and appears as isolated thin layers on the plane. The special type is mainly composed of mudstone and felsic siltstone, and mudstone, and turns up as lenses of different sizes on the plane.

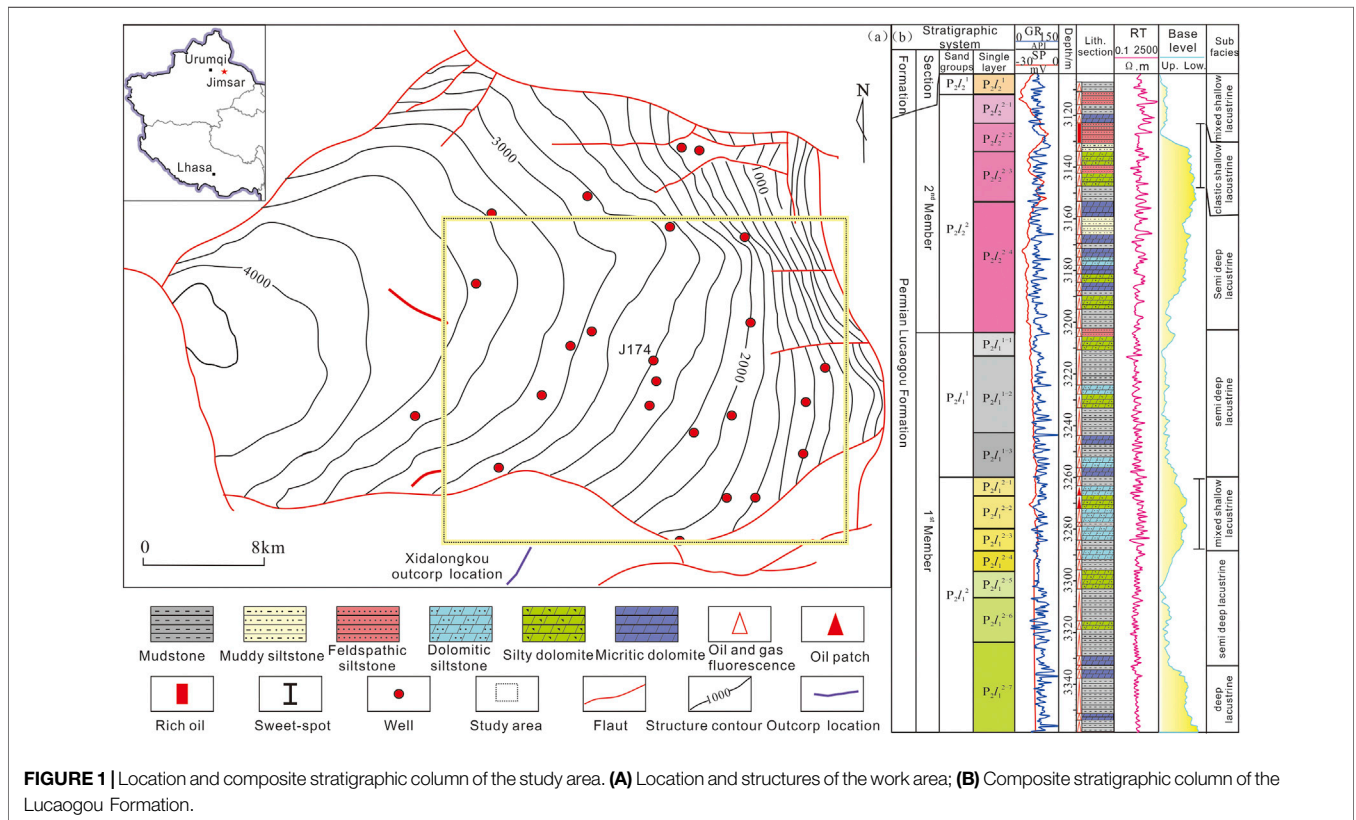
Keywords: mixed fine-grained rocks, lithofacies architecture, shale oil, UAV, sweet-spot, lucaogou formation, jimsar sag

INTRODUCTION

The combination and superimposition of different types of lithofacies in 3D spatial distribution is known as lithofacies architecture. In recent years, as the exploration and development of continental shale oil goes deeper (Yang et al., 2016; Du et al., 2019; Yang et al., 2019; Jin et al., 2019; Wei et al., 2020; Jia, 2020), fine-grained sedimentology related to shale lithofacies has gradually become a research hotspot (Yu et al., 2015; Yuan et al., 2015; Chen et al., 2017; Jin et al., 2020; Jiang et al., 2021). Further, as fine grains may experience different physical, chemical, and biological processes during the sedimentary and diagenetic stages, they may differ in structure and aggregation mode, coexistence process with organic matter, and diagenetic route, and thus the fine-grained rocks formed may differ widely in petrophysical properties and oil and gas storage capacity (Jiang et al., 2013; Xu et al., 2019, 2020a; Teng et al., 2020; Qiu et al., 2020; Dong et al., 2015). Therefore, study on lithofacies and features of lithofacies combinations of fine-grained rocks turns out to be more and more crucial (Bowker et al., 2007; Bohacs et al., 1998; Galvis et al., 2017; Liu et al., 2019; Xu et al., 2020b, 2020c). Generally speaking, from the perspective of evaluation and economic development of medium-high maturity shale oil (Zhao et al., 2020a; Zhao et al., 2020b), thin layers of coarser rocks (e.g., siltstone and dolomitic siltstone) (Zhang et al., 2012) sandwiched between thick mudstone layers are sweet-spot layers. Rocks of different lithofacies have wide differences in

geologic properties represented by the “7-petrophysical parameters” (Lu et al., 2018; Jin et al., 2021), and thus have different production features after fracturing.

Lithofacies architecture of continental shale oil reservoirs research has advanced in two aspects: lithofacies architecture classification of source-reservoir-in-one shale reservoirs, and lithofacies architecture of fine-grained shale reservoirs with rich organic matter (Zou et al., 2012; Zou et al., 2015). Firstly, from the perspective of shale oil accumulation, the source-reservoir combinations in shale strata are classified into three types, source-reservoir-in-one, reservoir separated from source, and pure shale; according to thermal evolution degree, shale strata are divided into two types, medium-high maturity (with Ro of over 1.0%) and low-medium maturity (with Ro of 0.5–1.0%) (Li et al., 2019; Fu et al., 2020; Zhao et al., 2020; Song et al., 2021). On this basis, the enrichment features and mechanisms of shale oil have been established. Secondly, lithofacies types and combinations of laminae, storage space features, and shale oil accumulation models in organic-rich shale strata have been revealed from core scale (Zhang et al., 2018; Zhu et al., 2019; Du et al., 2020). With wide differences in sedimentary, diagenetic, and reservoir-forming environments, different basins differ greatly in lithofacies combination, genetic mechanism, and a shale oil sweet-spot model. Although many studies on shale oil accumulation models at home and abroad have been reported, studies on lithofacies combinations and genetic mechanisms of mixed fine-grained rocks are rare. Therefore, it is urgent to analysis the heterogeneity in development scale, 3D





distribution features, and patterns of lithofacies in mixed fine-grained shale oil reservoirs.

GEOLOGICAL SETTING OF THE STUDY AREA AND RESEARCH METHODS

Geological Setting

Located in the east of Junggar Basin, Jimsar sag is a graben-shaped sag with a fault in the west and an overlap in the east developing

on the folded base of the Middle Carboniferous, where the strata thin from west to east (Figure 1A). In the Middle Permian, the study area was a lake near the sea, where intermittent invasion of sea water led to mass death of flora and fauna and a high development degree of organic matter. Deposited in a weakly reducing dysaerobic environment, the target layer, Lucaogou Formation is a set of mixed rocks formed by dolomitization in the penecontemporaneous stage, volcanism, and continental clast sedimentation (Ma et al., 2017; Li et al., 2020; Song et al., 2021; Zhi et al., 2021). It has an area of 1,278 km², a thickness of 50–160 m

TABLE 1 | Classification and origins of the rocks.

Lithofacies category	Lithofacies sub-category	Lithofacies type	Color and hydrodynamic description
Terrigenous clastic rocks	Mudstone(M)	Horizontal bedding mudstone M _h	Black, gray, with high clay mineral content, depositing in a quiet water body
		Laminar mudstone M _l	Black, with high clay mineral content, depositing in water with low hydrodynamics
	Felsic sandstone (FS)	Horizontal bedding feldspathic siltstone FS _h	Off-white, gray, formed in low hydrodynamic conditions
		Laminar feldspathic siltstone FS _l	Gray, brownish yellow, depositing in high hydrodynamic conditions
	Feldspathic siltstone(F)	Massive feldspathic siltstone FS _m	Mainly gray and blocky, formed in high hydrodynamic conditions
Mixed rocks	Dolomitic siltstone (DS)	Horizontal bedding dolomitic siltstone DS _h	Gray, blackish gray, depositing under high hydrodynamic conditions
		Laminar dolomitic siltstone DS _l	Blackish gray, with laminar texture, formed under low hydrodynamic conditions
		Massive dolomitic siltstone DS _m	Gray, blackish gray, depositing under high hydrodynamic conditions
	Silty dolomite (SD)	Laminar silty dolomite SD _l	Mainly blackish gray, depositing under low hydrodynamic conditions
Massive silty dolomite SD _m		Gray, blackish gray, formed under relatively high hydrodynamic conditions	
Carbonate rocks	Micritic/microcrystalline dolomite(D)	Horizontal bedding micritic/microcrystalline dolomite D _h	Black, gray, mostly with horizontal laminae, depositing under quiet water body conditions
		Laminar micritic/microcrystalline dolomite D _l	Mainly gray and massive, formed under high hydrodynamic conditions
		Massive micritic/microcrystalline dolomite D _m	Mainly black and blocky, indicating a low hydrodynamic depositional environment

(Figure 1), TOC of over 3.5%, mainly type II kerogen, and R_o of 0.6–1.1% in general. With dissolution pores, intercrystalline pores, and micro-fissures etc., it has a porosity range of 6–14%, an air permeability of less than $0.1 \times 10^{-3} \mu\text{m}^2$, an oil saturation range of 80–90%, and a brittle mineral content of over 85%. This Formation is divided into two members, Lu1 and Lu2, and four sand groups, P₁l₁¹, P₁l₁², P₂l₂¹, and P₂l₂² from bottom to top. The major reservoirs are two sweet-spot layers, the lower one (P₂l₁²) is mainly dolomitic siltstone; the upper one (P₂l₂²) is primarily composed of felsic siltstone, dolomitic siltstone, and silty dolomite (Figure 1B).

Research Methods

The West Dalongkou profile near the study area shows the Lucaogou Formation cropping out. Moreover, the study area has abundant development data, including data of 90 vertical wells and 30 horizontal wells, and coring data of 44 wells. Among the coring wells, three wells have cores of 600 m long in total taken from the whole Lucaogou Formation, providing sufficient test data. The lithofacies types, lithofacies combinations and patterns, and spatial distribution of lithofacies of the hybrid fine-grained rocks were examined by lithofacies hierarchy analysis, UAV photography outcrop modeling (Yin et al., 2021), and X-ray fluorescence (XRF) lithology identification using core, outcrop, logging, XRF element, and experimental assay data. The main steps are: ① different types of lithofacies were identified by core and thin section data, a UAV photography outcrop model, and XRF element analysis of core samples; ② lithofacies architecture patterns of the three kinds of typical hybrid fine-grained rocks in the study area were figured out by using outcrop and core data; ③ the lithology interpretation results from logging were used to figure out the distribution features

of lithofacies on the 3D space distribution patterns of mixed lithofacies in salty lacustrine facies.

RESULT AND DISCUSSION

Lithofacies Architecture and Lithofacies Combinations of the Mixed Fine-Grained Rocks

Lithofacies Types and Features of the Mixed Fine-Grained Rocks

Lucaogou Formation mixed rocks in the Jimsar sag are made up of clay minerals, carbonate minerals, and felsic minerals, and have average contents of plagioclase, potash feldspar, quartz, calcite, dolomite, ankerite, clay minerals, pyrite, and other minerals of 21.8, 3.6, 20.9, 11.9, 24.5, 1.7, 13.3, 0.9, and 1.4%, respectively. The rocks in the study area are largely black, grayish black, blackish gray, and gray, and have laminar, horizontal, and massive textures, etc.

According to lithology and sedimentary structure, the mixed fine-grained rocks are divided into 13 lithofacies types (including 8 clastic lithofacies and 5 carbonate lithofacies) in 5 sub-categories and 2 categories. Millimeter-scale lithologies can be observed directly on outcrops, but lithology identification of underground formations mainly relies on logging curves and cores. To make the study of combining underground formations and outcrops easier, the rocks were divided into five sub-categories of lithofacies in two categories in this work: mudstone, quartz siltstone, feldspar clastic sandstone, dolomitic siltstone, silty dolomite, and micritic dolomite (Figure 2). The mudstone (M) lithofacies includes horizontal bedding

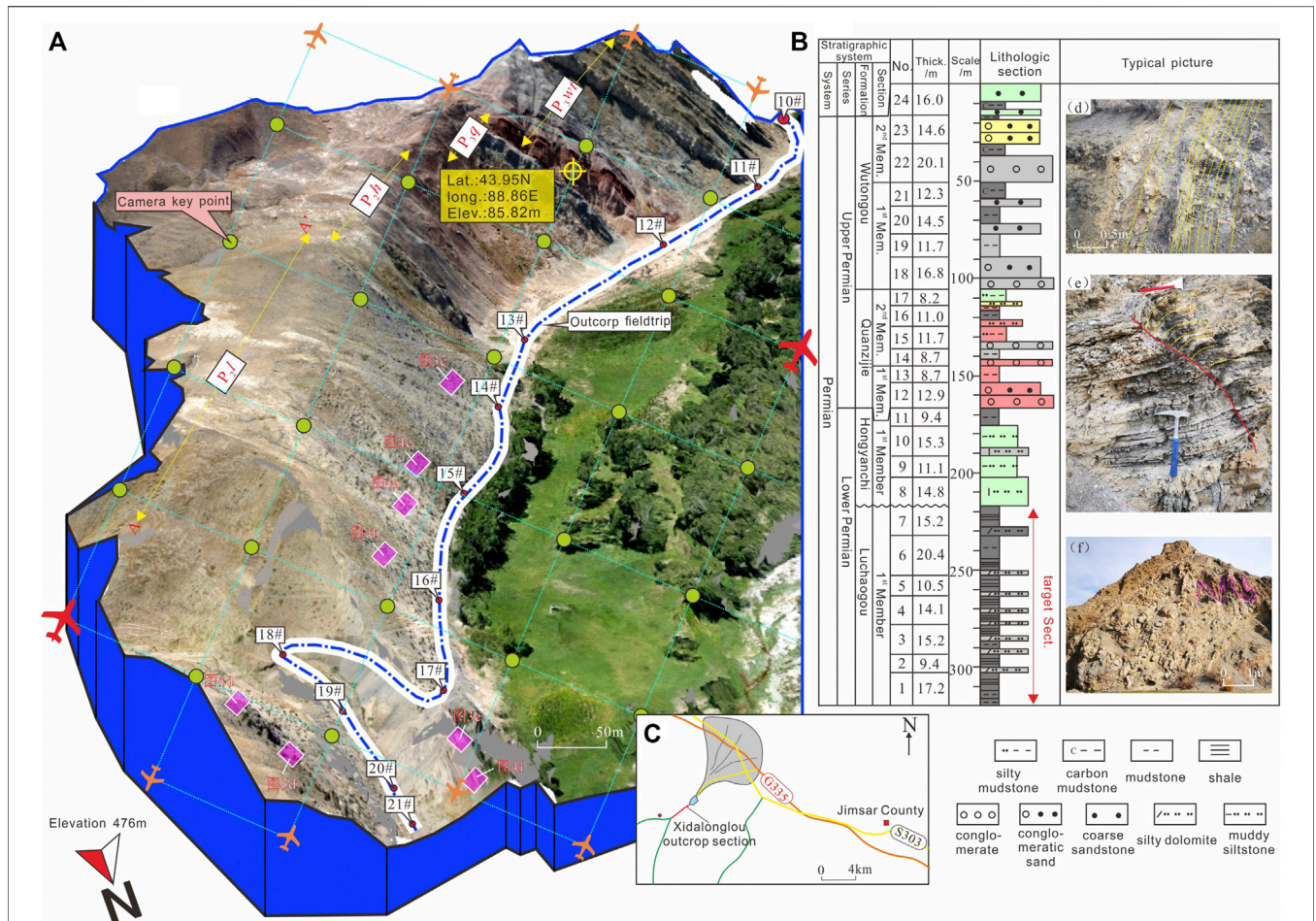


FIGURE 3 | Model and lithofacies distribution of Lucaogou Formation from 3D UAV photography. **(A)** UAV photography visualization model **(B)** Location of UAV data acquisition. **(C)** Lithology column of the target layer. **(D–F)** Representative lithofacies and sedimentary structures.

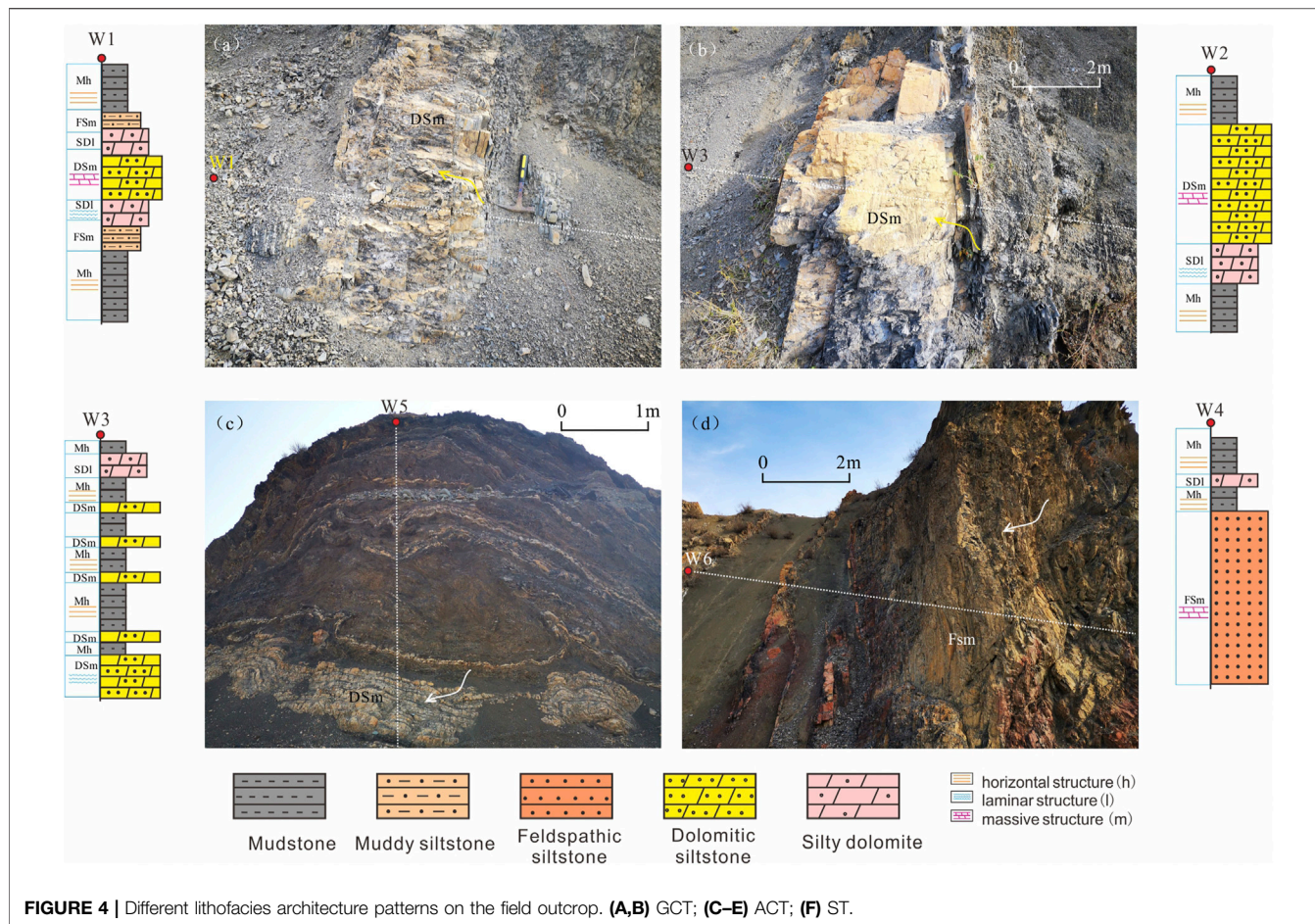
mudstone (M_h) and laminar mudstone (M_l). Quartz siltstone (S) and feldspar clastic siltstone (F) are called felsic siltstone (FS) in general, and include horizontal bedding felsic siltstone (FS_h), laminar felsic siltstone (FS_m), and massive felsic siltstone (FS_l). The dolomitic siltstone lithofacies (DS) includes horizontal bedding dolomitic siltstone (DS_h), massive dolomitic siltstone (DS_m), and laminar dolomitic siltstone (DS_l). The silty dolomite lithofacies (SD) includes massive silty dolomite (SD_m) and laminar silty dolomite (SD_l). The micritic dolomite lithofacies (D) consists of horizontal bedding micritic dolomite (D_h), laminar micritic dolomite (D_l), and massive micritic dolomite (D_m). The hydrodynamic environments of these types, sub-categories, and categories of lithofacies were described (Table 1). Different sub-categories of lithofacies have differences in lithology, porosity, and permeability, etc., which are reflected in the well logging. The mudstone (M) is characterized by a high value of GR and a low value of RXO on the conventional logging. Quartz siltstone (S) is characterized by a median GR, low AC, and a medium to high RXO on the conventional logging curve. The most typical feature of feldspathic siltstone (F) is that the GR value may be high due to potassium feldspar. The GR of the micrite/microcrystalline

dolomite (D) is the median value, the AC is the low value, and the RXO is the high value. The dolomitic siltstone (DS) and the silty dolomite (SD) are characterized by comprehensive characteristics based on the differences in the content of carbonate rocks and clastic rocks.

Lithofacies Architecture Combinations of the Mixed Fine-Grained Rocks

1) *Fine characterization of Lucaogou Formation rocks by UAV photography* Located 10 km west of Jimsar city of the Xinjiang region, the West Dalongkou profile is part of the nappe structural belt in the north margin of Mount Bogda. It connects to the Mount Karamay and Junggar basin to the east, and is very near to Mount Bogda and the Turpan-Hami basin to the south, with an altitude of about 1.1 km. Strata on the profile are continuous and turn from old to young from south to north, and have simple structures and diverse ancient animal fossils (Wei et al., 2018).

A UAV-carrying camera was used to collect outcrop data of the West Dalongkou profile, including high resolution photos



and positioning and orientating system (POS) data. The POS is an aerial photogrammetry system integrating dynamic GPS and an inertial navigation system, in which the spatial position of a photo is measured by the GPS, and the angular elements of a photo are measured by the gyroscopic system. The data collection was done by taking pictures at preset key photography points as the UAV flew along a preset route. After data collection, the point cloud data and pictures were processed, and the model after processing could pinpoint the 3D coordinates (longitude, latitude, and altitude) of any point in the outcrop area (Yin et al., 2018a; Yin et al., 2018b). The data collection covered an area of 0.6 km² and a profile about 716 m long and 123 m high at the resolution of 5–10 cm. Compared with the underground situation, the profile has only the Lu1 Member cropping out. The Lu1 Member is mainly composed of gray and grayish black shale and thin dolomitic siltstone interbeds of 0.2–0.5 m thick, and is 256 m long and 155 m thick on the profile. Due to strong compression of Mount Bogda and the soft nature of the rocks, it shows plastic slippage and has widespread crumpled structures (**Figures 3A,B**).

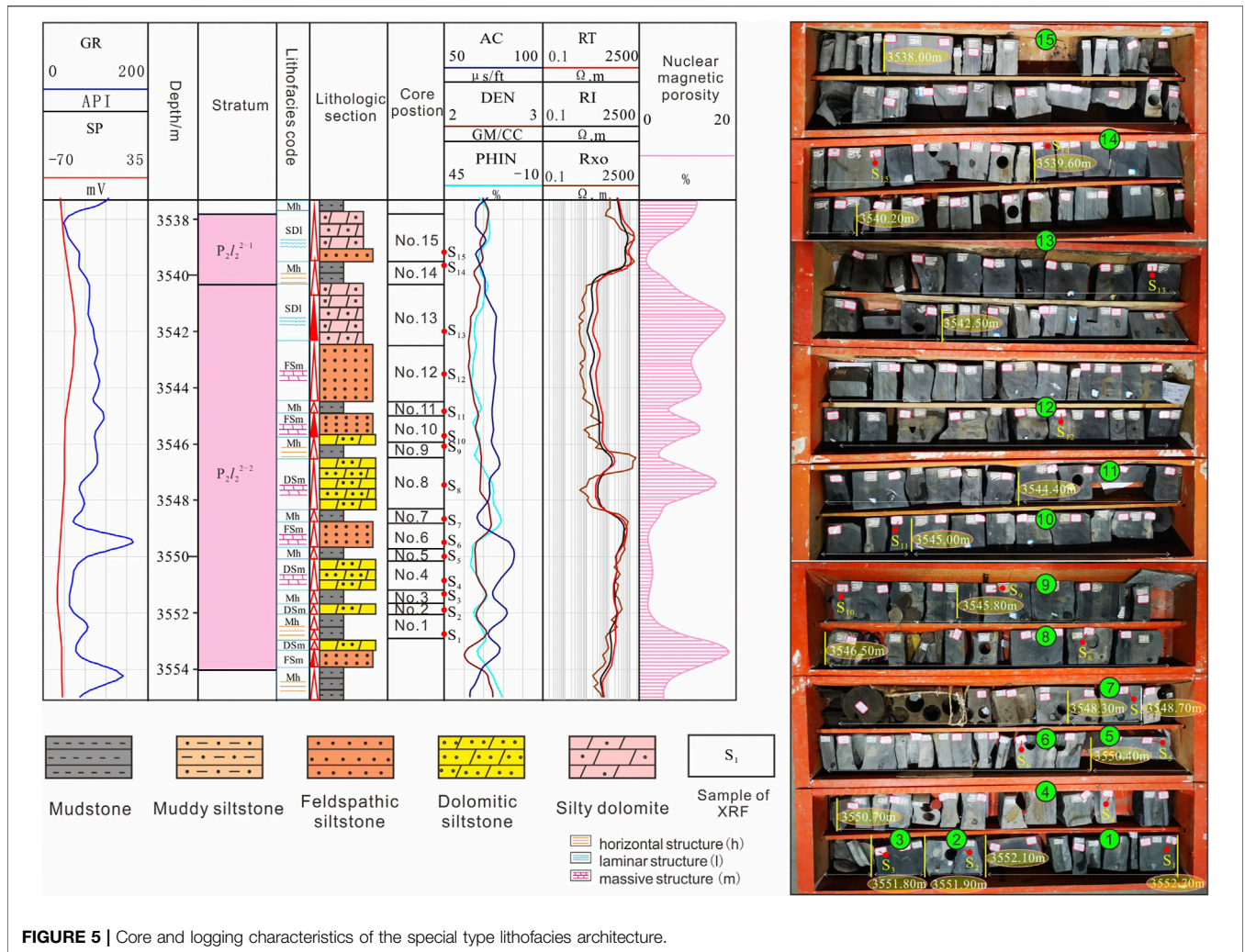
In the outcrop model obtained by UAV photography, the target consists of dark black, grayish black, blackish gray, gray, and in local parts grayish brown and grayish yellow mudstone laminae of 0.01–0.5 m thick. Horizontal bedding and massive DS are highly

developed, interbedded with shale layers, and are 0.2–1.5 m thick in single-layer and major-coarse lithofacies (**Figure 3C**).

2) *Lithofacies architecture types of the mixed fine-grained rocks*
According to detailed survey of the outcrop area and data of underground area of the Lucaogou Formation, the mixed fine-grained rocks have three types of typical lithofacies architecture patterns, gradual change, abrupt change, and special ones, which are quite different from each other.

① *Gradual Change Type (GCT)*

The GCT is composed of horizontal bedding mudstone, laminar felsic siltstone, horizontal bedding dolomitic siltstone, horizontal bedding felsic siltstone, and horizontal bedding mudstone ($M_h/M_h \rightarrow FS_1 \rightarrow DS_h \rightarrow FS_1 \rightarrow M_h/M_h$). This type of lithofacies combination has a better developed reservoir, symmetrical lithofacies architecture, source rock of about 8–10 m thick, and a reservoir layer of about 0.5–1.5 m thick (**Figures 4A,B**). The upper and lower mudstone layers (M_h) are thicker (about 1.5 m) and have source rock. In the lower part, the FS_1 thin layer of about 0.3–0.5 m, with high clay content, is a low quality reservoir. The DS_h layer, about 0.8 m thick, has low clay content and often dissolution pores, and is a high quality reservoir. The FS_1 and M_h



in the upper part are similar with those in the lower part. This type of lithofacies combination is the hybrid beach-bar sand formed in the mixed belt of hybrid shallow lake sub-facies, during the deposition of the hybrid beach-bar sand, the base level cycle rose rapidly first and then dropped slowly, and then rose slowly and dropped rapidly, forming the symmetrical depositional cycle. This kind of lithofacies architecture is commonly seen in the outcrop area and often comes in several similar cycles stacking over each other.

② *Abrupt Change Type (ACT)*

The ACT includes two kinds of lithofacies combinations. One is the combination of horizontal bedding micritic dolomite, horizontal bedding silty dolomite, and horizontal bedding micritic dolomite ($D_h \rightarrow SD_h \rightarrow D_h$), in which, the D_h with higher clay content is also the main source rock, whereas the SD_h is the reservoir. The other combination is horizontal bedding mudstone, horizontal bedding dolomitic siltstone, and horizontal bedding mudstone ($M_l/M_h \rightarrow DS_h \rightarrow M_l/M_h$), or occasionally the combination of horizontal bedding mudstone, laminar felsic

siltstone, and horizontal bedding mudstone ($M_l/M_h \rightarrow FS_l \rightarrow M_l/M_h$). This type of lithofacies architecture has an average sand development degree, asymmetrical architecture, a source rock layer of about 8–10 m, and a reservoir of about 0.5–1 m (Figure 4C). In the lower part of the combination, the mudstone (M_h) is generally in a thick layer of over 1.5 m and is the source rock; the SD_h comes in a thin layer of 0.3–0.5 m; the DS_h layer of about 0.5 m has low clay content and often dissolution pores, and thus is a high quality reservoir. The FS_l and M_h in the upper part are the same with those in the lower part. This type is dolomitic flat, formed in the mixed zone of hybrid shallow lake facies. During the deposition of dolomitic flat facies, the base level cycle rose rapidly and then fell slowly, resulting in the asymmetrical deposition cycle. This type of lithofacies architecture is commonly seen in the outcrop area, and often comes in several similar cycles stacking over each other.

③ *Special Type (ST)*

Besides these two types, there is a relatively independent type of lithofacies combination in the mixed zone, which is mainly

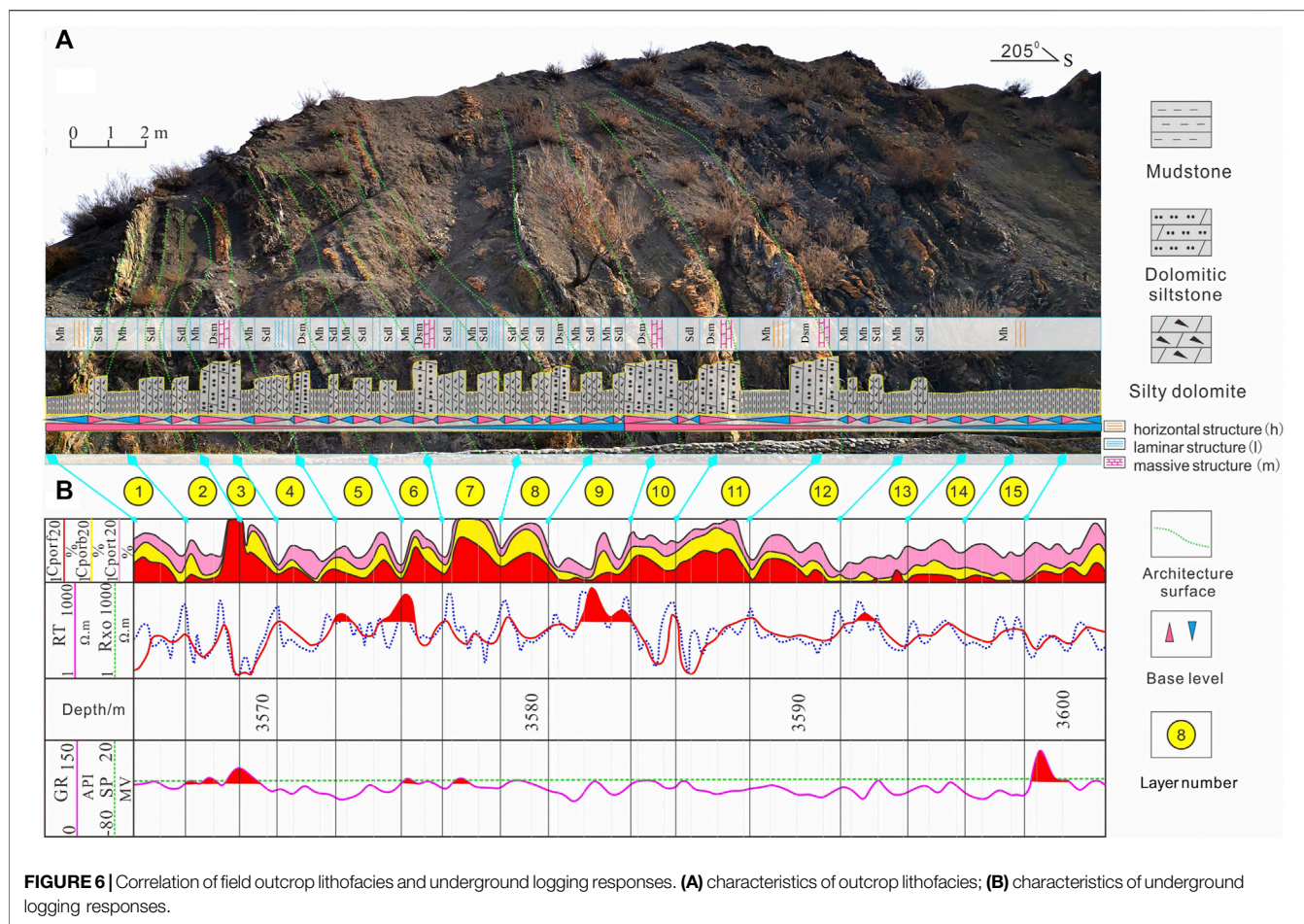
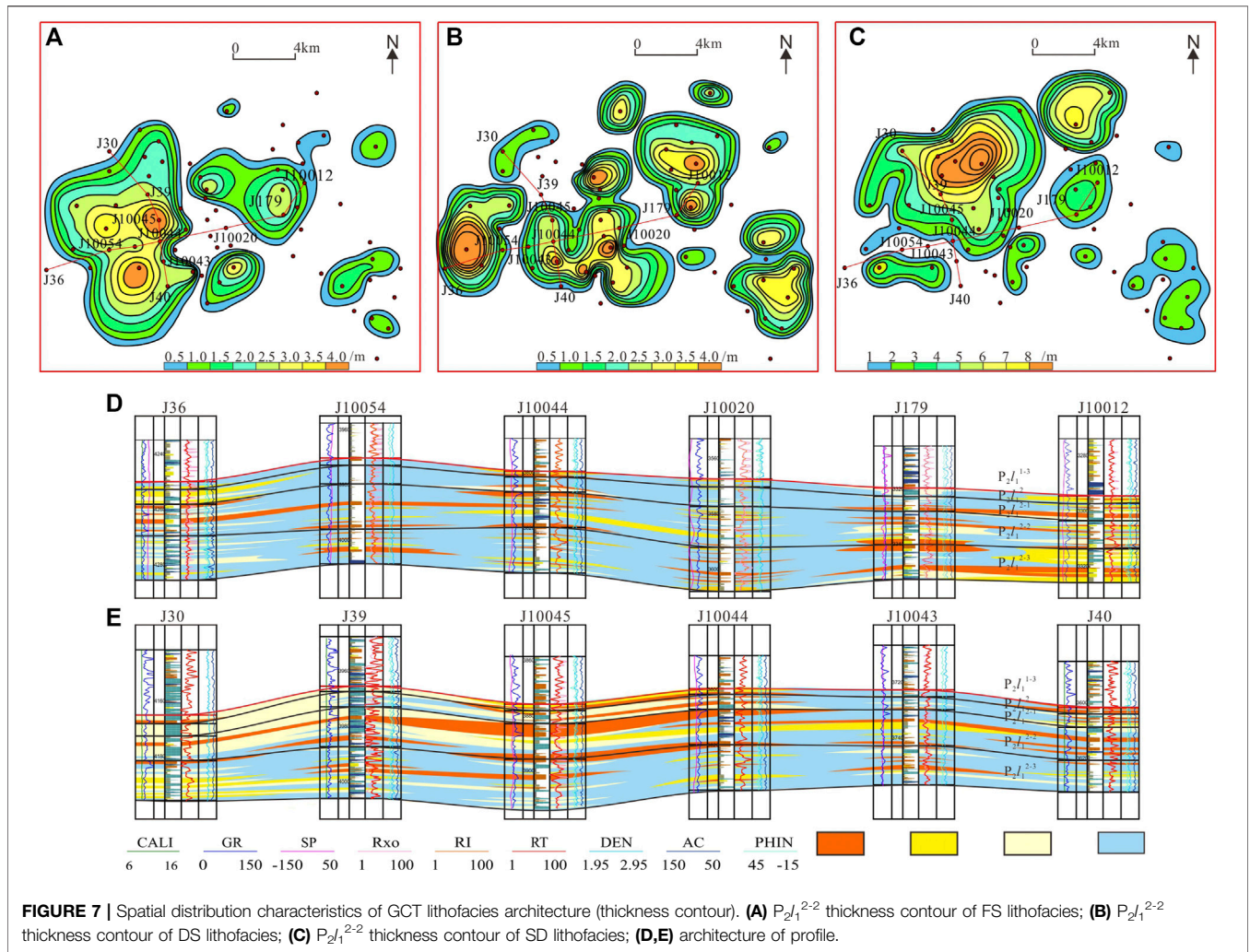


TABLE 2 | X-ray fluorescence logging of core samples.

XRF sample	MgO %	Al ₂ O ₃ %	SiO ₂ %	P ₂ O ₅ %	S %	Cl %	K ₂ O %	CaO %	TiO ₂ %	V %	MnO %	Fe ₂ O ₃ %	Rb %	Sr %	Ba %
S15	1.71	13.42	59.93	0.06	0.58	0.13	3.78	1.42	0.50	0.01	0.05	4.19	0.02	0.02	0.04
S14	1.82	15.03	63.43	0.06	0.10	0.23	4.33	1.43	0.51	0.01	0.06	4.68	0.02	0.01	0.06
S13	6.84	8.65	46.55	0.28	0.49	0.19	1.94	16.25	0.55	0.01	0.15	3.36	0.01	0.09	0.07
S12	4.03	7.87	51.74	0.71	0.16	1.88	1.41	13.71	0.49	0.01	0.18	4.20	0.01	0.09	0.07
S11	12.14	3.50	48.08	0.23	0.06	0.45	0.74	21.01	0.16	0.00	0.13	3.33	0.01	0.10	0.05
S10	12.11	3.52	41.72	0.22	0.14	0.33	0.64	23.09	0.18	0.00	0.12	2.86	0.01	0.13	0.08
S9	10.74	4.73	36.99	0.19	0.19	0.56	0.90	19.87	0.33	0.01	0.12	3.44	0.01	0.13	0.06
S8	3.59	9.23	51.63	0.12	0.10	0.34	1.54	12.57	0.40	0.01	0.13	3.93	0.01	0.06	0.07
S7	1.16	14.63	65.96	0.16	0.12	0.55	3.45	1.26	0.81	0.01	0.01	2.58	0.01	0.01	0.10
S6	4.65	12.10	63.00	0.11	0.10	0.07	2.67	6.91	0.65	0.01	0.08	3.25	0.01	0.04	0.08
S5	4.75	8.06	50.90	0.15	0.07	0.12	1.72	15.73	0.48	0.01	0.12	4.37	0.01	0.07	0.07
S4	5.69	8.03	54.29	0.18	0.05	0.32	1.74	15.05	0.39	0.01	0.12	4.56	0.01	0.07	0.06
S3	1.25	10.17	51.05	0.05	2.72	0.75	2.32	1.58	0.70	0.01	0.01	3.87	0.02	0.02	0.05
S2	4.43	8.06	59.81	0.13	0.58	0.17	1.73	10.70	0.35	0.00	0.09	2.65	0.01	0.07	0.06
S1	2.31	13.39	72.33	0.04	0.62	0.29	3.13	1.68	0.44	0.00	0.03	2.82	0.01	0.01	0.07

composed of fine clasts and is largely felsic silty sandstone. The ST is mainly composed of horizontal bedding/laminar mudstone, massive felsic siltstone, and horizontal bedding/laminar mudstone (M_l/M_h→FS_m→M_l/M_h). This combination has mainly clastic rock as the reservoir and a high sand development degree. The sand is thick-layered (3–8 m) massive feldspar clastic sandstone with muddy interlayers of unequal thicknesses (0.2–1.5 m), and is a higher

quality reservoir with properties of a tight reservoir (Figure 4C). The sand is sandwiched in between horizontal bedding or laminar mudstone source rock layers of about 0.5–1.5 m thick (Figure 5). This lithofacies combination is the typical shallow lake sand-bar of clastic shallow lake sub-facies, resulting from fast rise, fast drop, and fast rise again of the base level cycle. In the study area, this type of lithofacies architecture, as very thick clastic lithofacies, drew



attention first, and has been the major development object. The reservoir of this lithofacies architecture is close to a tight oil reservoir. Through logging curve calibration by cores, it has been confirmed that P_{2l}^{2-2} has muddy interlayers of about 0.2–0.5 m thick inside, sometimes, dividing the special thick layer into two 4–5 m thick feldspar clastic sandstone lithofacies.

Through XRF scanning of typical core sample points, element variations at different depths were characterized quantitatively to recognize the lithofacies type. Among the 15 scanning points in **Figure 6**, point S1 in section 1 is typical terrigenous clastic rock, with high *Si* and *Al* contents; point S2 in section 2 has an increase of *Mg* and *Ca* contents, indicating the increase of dolomite; point S3 in section 3 has an increase of *S* content, reflecting that pyrite content increases and the rock is shale-depositing in quiet bodies of water; section 4 is similar to section 2; section 5 is similar to S4 in element composition, but higher in dolomite, representing dolomitic mudstone; point S6 in section 6 is dominated by terrigenous clastic rock and has a relative increase of *K* and *Al*; sections 7, 9, 11, and 14 are similar to S3; point S8 in section 8 is similar to point S4; point S10 in section 10 has higher *Ca* and *Mg* contents, representing dolomitic siltstone, but the whole section was identified as felsic

siltstone through *GR* and *RXO* logging curves; point S12 in section 12 with an increase of *Al*, *K*, and *Si* contents is typical felsic siltstone, with a higher *P* content and a small amount of bioclasts; point S13 in section 13 with higher *Mg* and *Ca* contents is silty dolomite; point S15 in section 15 is typical terrigenous clastic rock (**Table 2**).

From the above analysis, it can be seen that the Lucaogou Formation in the outcrop has high comparability with that underground. The Lu1 Member of nearly 35 m underground can be correlated with the profile in the north of the outcrop area in 1–2 m small sweet spots (**Figure 5A**, **Figure 6**). From *RXO* and *CPOR* logging curves, gradual change and abrupt change lithofacies architectures can obviously be seen (**Figure 5B**). For example, the thick reservoir in the middle has a larger *CPOR* than layers above and below, this is shown as thick DS_h transitioning to the thin-layered SD_h above and below. Affected by the resolution of logging curves, a large number of 0.2–0.3 m thick reservoirs shown on the outcrop cannot be identified from logging curves, and these reservoirs are mostly of the abrupt change type in lithofacies architecture. For example, layer 3at a 3,570 m depth appears as an isolated bulge on the *CPOR* curve, which corresponds to abrupt changes of several thin layers on the outcrop (**Figure 5**).

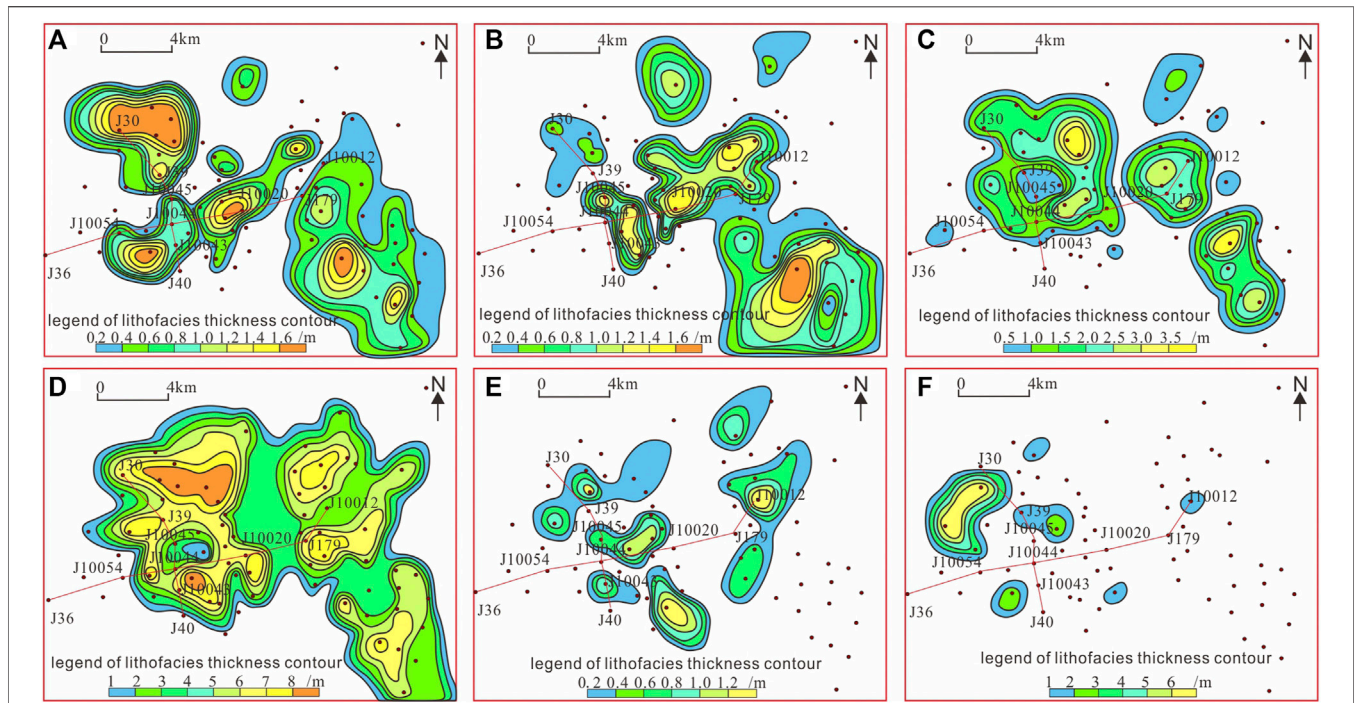


FIGURE 8 | Planar distribution characteristics of ACT and ST lithofacies architectures. **(A)** $P_{2l_2}^{2-1}$ thickness contour of FS lithofacies; **(B)** $P_{2l_2}^{2-1}$ thickness contour of DS lithofacies; **(C)** $P_{2l_2}^{2-1}$ thickness contour of SD lithofacies; **(D)** $P_{2l_2}^{2-2}$ thickness contour of FS lithofacies; **(E)** $P_{2l_2}^{2-2}$ thickness contour of DS lithofacies; **(F)** $P_{2l_2}^{2-2}$ thickness contour of SD lithofacies.

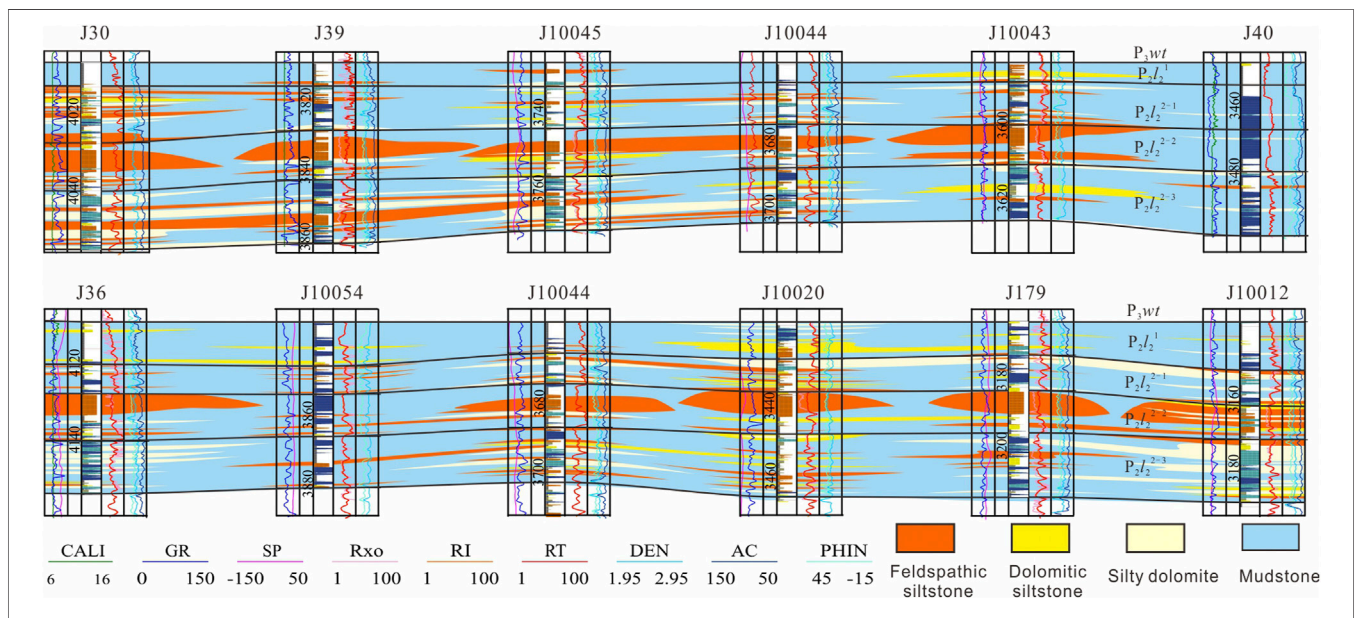


FIGURE 9 | Profile distribution characteristics of ACT and ST lithofacies architectures.

Spatial Distribution and Lithofacies Architecture Patterns of Mixed Fine-Grained Rocks

A planar thickness contour map of five types of lithofacies, mudstone facies (M), felsic siltstone facies (FS), dolomitic

siltstone facies (DS), silty dolomite facies (SD), and micrite/microcrystalline dolomite facies (D) in 80 wells of the work area was drawn. The FS, DS, and SD of the three lithofacies combinations have different distributions on the plane and profile, indicating strong heterogeneity of the mixed fine-grained rocks.

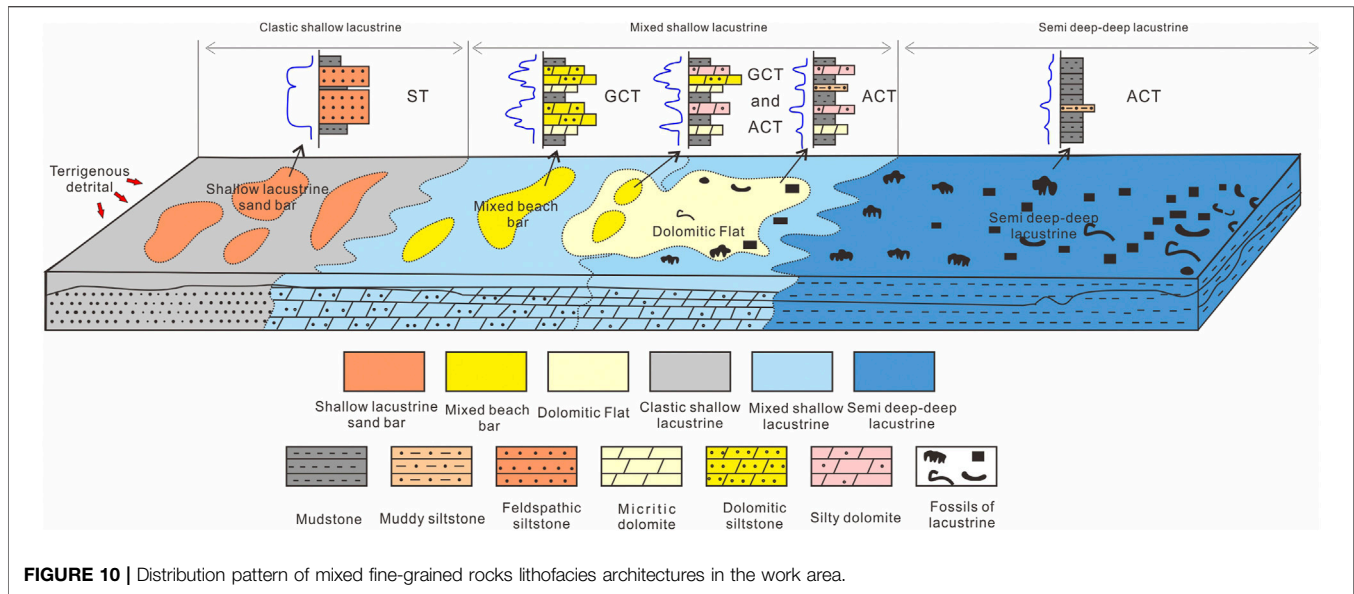


FIGURE 10 | Distribution pattern of mixed fine-grained rocks lithofacies architectures in the work area.

$P_2l_1^{2-2}$ as a representative of GCT is the major reservoir of the current shale oil development, and has mainly FS, DS, and SD lithofacies developing on the plane (Figure 7A). In this sand group, FS layers of 2.0–3.5 m thick occur mainly in two large contiguous pieces in the west and middle of the study area and are less developed in other areas; DS, in a 5–10 m thick layer that comes in four large contiguous pieces from west to east on the plane, is largest in area in the middle piece, but is scattered locally in the east part (Figure 7B); SD in a 2.5–4.5 m thick layer turns up in three to four large pieces on the plane and is contiguous in the west (Figure 7C). On the profile, the GCT lithofacies combination of mudstone to dolomitic siltstone to sandy dolomite to dolomitic siltstone to mudstone (M→DS→SD→DS→M) takes dominance, and is mainly distributed in the middle and northwest areas (Figures 7D,E). The combination M→FS→SD→FS→M also exists, and is mainly distributed in the west and southwest of the work area. These three reservoir lithofacies mainly stack in the north-central and southeast areas.

$P_2l_2^{2-1}$ is representative of ACT and the replacement domain for shale oil development. In this sand group, the FS, DS, and SD are different in distribution location, and thin, isolated, and larger in distribution range on the plane; while sandy coarse grain parts of them seldom stack on the profile. Most of the combinations have coarse grains in the middle and ACT above and below (Figure 8A). The FS layers, with thicknesses from 0.4 to 1.4 m (0.8 m on average) mostly turn up in isolated patches in the northwest, middle, and southeast areas (Figure 8B). The DS layers, 0.4–1.2 m thick, 0.6 m on average, mainly appear as isolated contiguous patches in the middle and southeast areas (Figure 8C). The SD layers 1.0–2.5 m thick, on average 1.5 m, come up in isolated contiguous patches in the central and northwestern areas. On the profile, felsic siltstone facies, dolomitic siltstone facies, sandy dolomite facies, and mudstone facies (M→FS→M, M→SD→M, M→SD→M) superimpose, and come in thin isolated layers.

$P_2l_2^{2-2}$ as a representative of the ST is the major target for early shale oil development. In this sand group, FS layers are 5–10 m

thick, 6 m on average, and have dispersed distribution (Figure 8D); DS layers are 0.4–1.0 m thick, on average 0.5 m, and mainly come up in isolation in the middle of the study area (Figure 8E); SD layers of this type are 1.0–3.0 m thick, on average 1.5 m, and mostly appear as isolated layers in the west (Figure 8F). DS and SD are less developed. On the profile, the lithofacies combination from mudstone to felsic siltstone to mudstone (Mh→FSm→Mh) is most common, and FS and SD superimpose in local parts; this type in lenticular shape appear in isolation mostly in the middle and central-east parts, and less in the east and west (Figure 9).

Lithofacies Architecture Patterns of the Mixed Fine-Grained Rocks

Any kind of lithofacies contains dolomite, leading to the interbedding of mixed fine-grained rocks and organic-rich shale, forming a characteristic distribution pattern of mixed fine-grained rocks architecture. Affected by the changes of base level cycles, lithofacies architecture has obvious zonation and differentiation in spatial distribution, and shows an overall evolution trend from shallow clastic lacustrine to hybrid shallow lacustrine to semi-deep lacustrine facies. The clastic shallow lacustrine sediments have mainly terrigenous clastic particles as source material, thick-layered FS of the special lithofacies architecture, and scattered distribution over a large range on the plane. In contrast, the hybrid shallow lacustrine sediments are a mixture of terrigenous clastic materials and dolomite, with a hybrid beach bar in a potato shape in a limited range, and have mainly GCT and symmetrical lithofacies architecture of DS and SD. Toward the deep water, dolomitic flat spreads in the sheet, in which the ACT of lithofacies architecture with SD as the reservoir takes dominance. The hybrid beach bar and dolomitic flat sometimes superimpose over each other, forming the GCT of lithofacies architecture (Figure 10).

CONCLUSION

Through the above study, we have reached the following conclusions:

- 1) According to lithology and sedimentary structure, the mixed fine-grained rocks can be divided into 13 lithofacies types (including 8 types of clastic lithofacies and 5 types of carbonates lithofacies) in 5 sub-categories and 2 categories. The origins and features of different lithofacies types in the study area were analyzed.
- 2) UAV photography was combined with a traditional field survey to characterize the lithofacies architectures of the Lucaogou Formation on the outcrop, and it is found that the lithofacies architecture combinations of mixed fine-grained rocks include three types: GCT, ACT, and ST. The GCT with higher sand development degree and symmetrical lithofacies architecture has a high quality reservoir with dissolution pores, and is mixed beach-bar sand in the mixed zone. This type is high in development degree and often appears as several similar cycles stacking over each other. The ACT can be subdivided into two sub-types, is average in sand development degree, asymmetric, and smaller in reservoir thickness. This type is very high in development degree and often comes in several similar cycles. The ST belongs to thick clastic rock, relatively independent in the mixed fine-grained rocks with a high development degree of sand. Its combination is thick-layer FSm, which is a higher quality reservoir with properties of a tight reservoir. And this type often appears as stacking of single-cycle sand layers.
- 3) In the distribution of mixed fine-grained rocks of different lithofacies architectures, different layers differ widely in

lithofacies architecture. The GCT represented by $P_2l_1^{2-2}$ has the architecture pattern of $M \rightarrow DS \rightarrow SD \rightarrow DS \rightarrow M$ and appears as a limited lens overlapping on the plane. The ACT represented by $P_2l_2^{2-1}$ has the architecture patterns of $M \rightarrow FS \rightarrow M$, $M \rightarrow SD \rightarrow M$ and $M \rightarrow SD \rightarrow M$ and appears as isolated thin layers on the plane. The ST represented by $P_2l_2^{2-2}$ has the architecture pattern of $M_h \rightarrow FS_m \rightarrow M_h$ and turns up as a lens of different sizes on the plane.

DATA AVAILABILITY STATEMENT

The original contributions presented in the study are included in the article/Supplementary Material, further inquiries can be directed to the corresponding authors.

AUTHOR CONTRIBUTIONS

SY, YW, and BZ designed the research. SY wrote the manuscript. BZ discussed the results. YW and FX performed data analyses. YW prepared the figures and tables.

FUNDING

This work was supported by the National Major Science and Technology Project (No. 2017ZX05008-006-004-002) and Geological Resources and Geological Engineering Top Discipline Subject Open Fund Project of Yangtze University No (2019KFJJ0818022).

REFERENCES

- Bohacs, K. M. (1998). "Introduction: Mud Rock Sedimentology and Stratigraphy—Challenges at the basin to Local Scales," in *Shales and Mudstones: Basin studies* [J]. *Sedimentology and Paleontology*. Editors J. Schieber, W. Zimmerle, and P. Sethi (Stuttgart: Schweizerbart'sche Verlagsbuchhandlung), 1, 13–20. doi:10.2110/jsr.2018.69
- Bowker, K. A. (2007). Barnett Shale Gas Production, Fort Worth Basin: Issues and Discussion. *AAPG Bull.* 91 (4), 523–533. doi:10.1306/06190606018
- Chen, S., Zhang, S., Liu, H., and Yan, J. (2017). Discussion on Mixing of fine-grained Sediments in Lacustrine Deep Water. *J. J. Palaeogeogr.* 19 (2), 271–284. doi:10.7605/gdxb.2017.02.021
- Dong, C., Ma, C., Lin, C., Sun, X., and Yuan, M. (2015). A Method of Classification of Shale Set. *J. J. China Univ. Pet. (Edition Soc. Sciences)* 39 (3), 1–7. doi:10.3969/j.issn.1673-5005.2015.03.001
- Du, J., Hu, S., Pang, Z., Lin, S., Hou, L., and Zhu, R. (2019). The Types, Potentials and Prospects of continental Shale Oil in China. *J. China Pet. Exploration* 24 (5), 560–568. doi:10.3969/j.issn.1672-7703.2019.05.003
- Du, X., Liu, X., Lu, Y., Liu, H., Zhang, S., Ma, Y., et al. (2020). Classification, Characteristics and Development Models of continental fine-grained Mixed Sedimentation: a Case Study of Dongying Sag. *J. Acta Petrolei Sinica.* 41 (11), 1324–1333. doi:10.7623/syxb202011003
- Fu, J., Li, S., Niu, X., Deng, X., and Zhou, X. (2020). Geological Characteristics and Exploration of Shale Oil in Chang 7 Member of Triassic Yanchang Formation, Ordos Basin, NW China. *J. Pet. Exploration Develop.* 47 (5), 870–883. doi:10.11698/PED.2020.05.03
- Galvis, H., Becerra, D., and Slatt, R. (2018). Lithofacies and Stratigraphy of a Complete Woodford Shale Outcrop Section in South Central Oklahoma: Geologic Considerations for the Evaluation of Unconventional Shale Reservoirs. *Interpretation* 6 (1), 15–27. doi:10.1190/INT-2017-0074.1
- Jia, C. (2020). Development Challenges and Future Scientific and Technological Researches in China's Petroleum Industry Upstream. *J. Acta Petrolei Sinica.* 41 (12), 1445–1464. doi:10.7623/syxb202012001
- Jiang, Z., Kong, X., Yang, Y., Zhang, J., Zhang, Y., Wang, L., et al. (2021). Multi-source Genesis of continental Carbonate-Rich fine-grained Sedimentary Rocks and Hydrocarbon Sweet Spots. *J. Pet. Exploration Develop.* 48 (1), 1–12. doi:10.11698/PED.2021.01.03
- Jiang, Z., Liang, C., Wu, J., Zhang, J., Zhang, W., Wang, Y., et al. (2013). Several Issues in Sedimentological Studies on Hydrocarbon-Bearing fine-grained Sedimentary Rocks. *J. Acta Petrolei Sinica.* 34 (6), 1031–1039. doi:10.7623/syxb201306001
- Jin, X., Li, G., Meng, S., Wang, X., Liu, C., Tao, J., et al. (2021). Microscale Comprehensive Evaluation of continental Shale Oil Recoverability. *J. Pet. Exploration Develop.* 48 (1), 1–11. doi:10.11698/PED.2021.01.21
- Jin, Z., Bai, Z., Gao, B., and Li, M. (2019). Has China Ushered in the Shale Oil and Gas Revolution?. *J. Oil Gas Geology.* 40 (3), 451–458. doi:10.11743/ogg20190301
- Jin, Z., Tan, X., Tang, H., Shen, A., Qiao, Z., Zheng, J., et al. (2020). Sedimentary Environment and Petrological Features of Organic-Rich fine Sediments in Shallow Water Overlapping Deposits: A Case Study of Cambrian Yuertus Formation in Northwestern Tarim Basin, NW China. *J. Pet. Exploration Develop.* 47 (3), 476–489. doi:10.11698/PED.2020.03.04
- Li, M., Ma, X., Jiang, Q., Li, Z., Pang, X., and Zhang, C. (2019). Enlightenment from Formation Conditions and Enrichment Characteristics of marine Shale Oil in North America. *J. Pet. Geology. Recovery Efficiency* 26 (1), 13–28. doi:10.13673/j.cnki.cn37-1359/te.2019.01.002
- Li, S., Yin, S., Gao, Y., Zhang, F., Li, Y., and Peng, S. (2020). Study on Sedimentary Microfacies of Mixed fine-grained Rocks in Lucaogou Formation, Jimsar

- SagJunggar Basin. *J. Nat. Gas Geosci.* 31 (02), 235–249. doi:10.11764/j.issn.1672-1926.2019.11.002
- Liu, B., Wang, H., Fu, X., Bai, Y., Bai, L., Jia, M., et al. (2019). Lithofacies and Depositional Setting of a Highly Prospective Lacustrine Shale Oil Succession from the Upper Cretaceous Qingshankou Formation in the Gulong Sag, Northern Songliao Basin, Northeast China. *AAPG Bull.* 103 (2), 405–432. doi:10.1306/08031817416
- Lu, S., Li, J., Zhang, P., Xue, H., Wang, G., Zhang, J., et al. (2018). Classification of Microscopic Pore-Throats and the Grading Evaluation on Shale Oil Reservoirs. *J. Pet. Exploration Develop.* 45 (3), 1–9. doi:10.11698/PED.2018.03.08
- Ma, K., Hou, J., Liu, Y., Shi, Y., Yan, L., and Chen, F. (2017). The Sedimentary Model of saline Lacustrine Mixed Sedimentation in Permian Lucaogou Formation, Jimsar Sag. *J. Acta Petrolei Sinica.* 38 (6), 636–648. doi:10.7623/syxb201706003
- Qiu, Z., and Zou, C. (2020). Unconventional Petroleum Sedimentology: Connotation and Prospec. *J. Acta Sedimentologica Sinica.* 38 (1), 1–29. doi:10.14027/j.issn.1000-0550.2019.116
- Song, Y., Luo, Q., Jiang, Z., Yang, W., and Liu, D. (2021). Enrichment of Tight Oil and its Controlling Factors in central and Western China. *J. Pet. Exploration Develop.* (2), 1–13. doi:10.11698/PED.2021.02.19
- Teng, J., Liu, H., Qiu, L., and Zhang, S. (2020). Sedimentary and Diagenetic Characteristics of Lacustrine Fine-Grained Hybrid Rock in Paleogene Formation in Dongying Sag. *J. Earth Sci.* 45 (10), 3807–3826. doi:10.3799/dqkx.2020.127
- Wei, L. (2018). *Remote Sensing Interpretation and Application of Sedimentary Lithology—A Case Study in Jimsar District of Xinjiang*. D. Shanxi Xi'an: Northwest University. CNKI:CDMD:2.1018 104857
- Wei, Y., Wang, H., Liu, D., Zhao, Q., Zheng, M., and Wang, S. (2021). Probing and Thinking on “Exploring Petroleum inside Source Kitchen” of Continental Shale Oil Exploration—A Case Study of the First Member of Shahejie Formation in Qikou Sag, Bohai Bay Basin, China. *J. J. Earth Sci. Environ.* 43 (1), 117–134. doi:10.19814/j.jese.2020.10038
- Xu, S., Gou, Q., Hao, F., Zhang, B., Shu, Z., Lu, Y., et al. (2020c). Shale Pore Structure Characteristics of the High and Low Productivity wells, Jiaoshiba Shale Gas Field, Sichuan Basin, China: Dominated by Lithofacies or Preservation Condition. *Mar. Pet. Geology.* 114, 104211. doi:10.1016/j.marpetgeo.2019.104211
- Xu, S., Hao, F., Shu, Z., Zhang, A., and Yang, F. (2020b). Pore Structures of Different Types of Shales and Shale Gas Exploration of the Ordovician Wufeng and Silurian Longmaxi Successions in the Eastern Sichuan Basin, South China. *J. Asian Earth Sci.* 193, 104271. doi:10.1016/j.jseaes.2020.104271
- Xu, S., Hao, F., Zhang, Y., and Gou, Q. (2020a). High-quality marine Shale Reservoir Prediction in the Lower Silurian Longmaxi Formation, Sichuan Basin, China. *Interpretation* 8 (2), T453–T463. doi:10.1190/int-2019-0149.1
- Xu, S., Liu, R., Hao, F., Engelder, T., Yi, J., Zhang, B., et al. (2019). Complex Rotation of Maximum Horizontal Stress in the Wufeng-Longmaxi Shale on the Eastern Margin of the Sichuan Basin, China: Implications for Predicting Natural Fractures. *Mar. Pet. Geology.* 109, 519–529. doi:10.1016/j.marpetgeo.2019.06.008
- Yang, H., Niu, X., Xu, L., Feng, S., Yuan, Y., Xiao, W., et al. (2016). Exploration Potential of Shale Oil in Chang 7 Member, Upper Triassic Yanchang Formation, Ordos Basin, NW China. *J. Pet. Exploration Develop.* 43 (4), 511–520. doi:10.11698/PED.2016.04.02
- Yang, Z., and Zou, C. (2019). “Exploring Petroleum inside Source Kitchen”: Connotation and Prospects of Source Rock Oil and Gas. *J. Pet. Exploration Develop.* 46 (1), 173–184. doi:10.11698/PED.2019.01.18
- Yin, S., Chen, G., Liu, Z., Feng, W., and Liu, Y. (2018a). 3D Digital Outcrop Characterization Technology Based on Unmanned Aerial Vehicle Oblique Photography. *J. Acta Sedimentologica Sinica.* 36 (1), 72–80. doi:10.3969/j.issn.1000-0550.2018.009
- Yin, S., Gao, Y., Hu, Z., Xiong, T., Feng, W., Zhao, J., et al. (2021). Multiple-point Geostatistical Simulation of Outcrop Based on UAV Oblique Photographic Data: A Case Study of Shihezi Formation in Pingtuo township, Lvliang city, Shanxi. *J. Acta Petrolei Sinica.* 42 (02), 198–216. doi:10.7623/syxb202102005
- Yin, S., Tan, Y., Zhang, L., Feng, W., Liu, S., and Jin, J. (2018b). 3D Outcrop Geological Modeling Based on UAV Oblique Photography Data: A Case Study of Pingtouxiang Section in Lüliang City, Shanxi Province. *J. J. Palaeogeogr.* 20 (5), 909–924. doi:10.7605/gdxb.2018.05.064
- Yu, X., Li, S., and Yang, Z. (2015). Discussion on Deposition-Diagenesis Genetic Mechanism and Hot Issues of Tight sandstone Gas Reservoir. *J. Lithologic Reservoirs* 27 (1), 1–14. doi:10.3969/j.issn.1673-8926.2015.01.001
- Yuan, X., Lin, S., Liu, Q., Yao, J., Wang, L., Guo, H., et al. (2015). Lacustrine fine-grained Sedimentary Features and Organic-Rich Shale Distribution Pattern: A Case Study of Chang 7 Member of Triassic Yanchang Formation in Ordos Basin, NW China. *J. Pet. Exploration Develop.* 42 (1), 34–43. doi:10.11698/PED.2015.01.04
- Zhang, J., Lin, L., Li, Y., Tang, X., Zhu, L., Xing, Y., et al. (2012). Classification and Evaluation of Shale Oil. *J. Earth Sci. Front.* 19 (5), 322–331.
- Zhang, S., Cao, Y., Zhu, R., Xi, K., Wang, J., Zhu, N., et al. (2018). Lithofacies Classification of fine-grained Mixed Sedimentary Rocks in the Permian Lucaogou Formation, Jimsar Sag, Junggar Basin. *J. Earth Sci. Front.* 25 (04), 198–209. doi:10.13745/j.esf.yx.2017-5-2
- Zhao, W., Hu, S., Hou, L., Yang, T., Li, X., Guo, B., et al. (2020a). Types and Resource Potential of continental Shale Oil in China and its Boundary with Tight Oil. *Pet. Exploration Develop.* 47 (1), 1–11. doi:10.11698/PED.2020.01.01
- Zhao, W., Zhu, R., Hu, S., Hou, L., and Wu, S. (2020b). Accumulation Contribution Differences between Lacustrine Organic-Rich Shales and Mudstones and Their Significance in Shale Oil Evaluation. *J. Pet. Exploration Develop.* 47 (6), 1079–1089. doi:10.11698/PED.2020.06.02
- Zhao, Z., Zhou, L., Pu, X., Jin, F., Shi, Z., Han, W., et al. (2020). Formation Conditions and Enrichment Model of Retained Petroleum in Lacustrine Shale: A Case Study of the Paleogene in Huanghua Depression, Bohai Bay Basin, China. *J. Pet. Exploration Develop.* 47 (5), 856–869. doi:10.11698/PED.2020.05.02
- Zhi, D., Tang, Y., He, W., Guo, Y., Zheng, M., Huang, L., et al. (2021). Orderly Coexistence and Accumulation Models of Conventional and Unconventional Hydrocarbons in Lower Permian Fengcheng Formation, Mahu sag, Junggar Basin. *J. Pet. Exploration Develop.* 48 (1), 38–51. doi:10.11698/PED.2021.01.04
- Zhu, B., Tang, H., Wang, X., Zhao, F., and Yuan, X. (2019). Coupled CFD-DEM Simulation of Granular LCM Bridging in a Fracture. *Particul. Sci. Technol.*, 1–10.
- Zou, C., Tao, S., Bai, B., Yang, Z., Zhu, R., Hou, L., et al. (2015). Differences and Relations between Unconventional and Conventional Oil and Gas. *J. China Pet. Exploration* 20 (1), 1–16. doi:10.3969/j.issn.1672-7703.2015.01.001
- Zou, C., Yang, Z., Tao, S., Li, W., Wu, S., Hou, L., et al. (2012). Nano-hydrocarbon and the Accumulation in Coexisting Source and Reservoir. *J. Pet. Exploration Develop.* 39 (1), 13–26. Available at: <http://www.cpedm.com/CN/Y2012/V39/I1/2> doi:10.1016/s1876-3804(12)60011-1

Conflict of Interest: FX was employed by the company PetroChina Xinjiang Oilfield Company.

The remaining authors declare that the research was conducted in the absence of any commercial or financial relationships that could be construed as a potential conflict of interest.

Publisher's Note: All claims expressed in this article are solely those of the authors and do not necessarily represent those of their affiliated organizations, or those of the publisher, the editors and the reviewers. Any product that may be evaluated in this article, or claim that may be made by its manufacturer, is not guaranteed or endorsed by the publisher.

Copyright © 2021 Yin, Zhu, Wu and Xu. This is an open-access article distributed under the terms of the Creative Commons Attribution License (CC BY). The use, distribution or reproduction in other forums is permitted, provided the original author(s) and the copyright owner(s) are credited and that the original publication in this journal is cited, in accordance with accepted academic practice. No use, distribution or reproduction is permitted which does not comply with these terms.